28. An optimized Schwarz method in the Jacobi-Davidson method for eigenvalue problems

M. Genseberger[1], G. L. G. Sleijpen[2], and H. A. van der Vorst[3]

1. Introduction. The Jacobi-Davidson method [3] is an iterative method suitable for the computation of solutions to large scale (generalized) eigenvalue problems. Most of the computational work of the Jacobi-Davidson method arises from performing (approximate) solves for the so-called correction equation. In order to relieve this amount of work and/or the local memory requirements we propose a strategy based on domain decomposition.

The domain decomposition method is based on previous work for ordinary systems of (definite) linear equations (§3). It requires specific knowledge of the underlying PDE's. For eigenvalue problems the situation is more complex as the correction equation is (highly) indefinite. In this paper we describe and analyze the situation for the correction equation (§4). Results of the analysis are of practical interest for more general cases like PDE's with variable coefficients, many subdomains in two directions and complex geometries (§5). The proposed domain decomposition approach enables a massively parallel treatment of large scale eigenvalue problems ([1, §4]).

2. The Jacobi-Davidson method. The Jacobi-Davidson method [3] projects the original eigenvalue problem on a suitable search subspace. From the projected eigenvalue problem approximate solutions to the original problem are computed. The search subspace is expanded iteratively with the most important direction in the residual not already present. Compared to other methods the Jacobi-Davidson method offers many advantages and flexibility such as the exploitation of a good preconditioner.

For a standard eigenvalue problem $\mathbf{A}\,\mathbf{x} = \lambda\,\mathbf{x}$ each iteration step Jacobi-Davidson

- **extracts** an approximate solution $(\theta, \mathbf{u}) \approx (\lambda, \mathbf{x})$ from a search subspace

  > construct $H \equiv \mathbf{V}^* \mathbf{A}\,\mathbf{V}$,
  >
  > solve $H\,s = \theta\,s$, and compute $\mathbf{u} = \mathbf{V}\,s$
  >
  > where the columns of $\mathbf{V}$ form an orthonormal basis for the search subspace

- **corrects** the approximate eigenvector $\mathbf{u}$

  > compute a correction $\mathbf{t}$ from the *correction equation*:
  >
  > $\mathbf{t} \perp \mathbf{u}, \quad \mathbf{P}\,\mathbf{B}\,\mathbf{P}\,\mathbf{t} = \mathbf{r}$
  >
  > where $\mathbf{P} \equiv \mathbf{I} - \frac{\mathbf{u}\,\mathbf{u}^*}{\mathbf{u}^*\mathbf{u}}$, $\mathbf{B} \equiv \mathbf{A} - \theta\,\mathbf{I}$, and $\mathbf{r} \equiv -\mathbf{B}\,\mathbf{u}$

- **expands** the search subspace with the correction $\mathbf{t}$

  > $\mathbf{V}_{new} = \begin{bmatrix} \mathbf{V} \,|\, \mathbf{t}^\perp \end{bmatrix}$
  >
  > where $\mathbf{t}^\perp = \alpha\,(\mathbf{I} - \mathbf{V}\,\mathbf{V}^*)\,\mathbf{t}$ such that $\|\mathbf{t}^\perp\|_2 = 1$

3. An optimized Schwarz method. For the domain decomposition technique we adapt a locally optimized additive Schwarz method based on work by Tan & Borsboom [5, 4] for linear systems which in its turn is a generalization of work by Tang [6]. We show the main ingredients and discuss some details for ordinary linear systems. The situation for the correction equation is described and analysed in §4.

[1]Utrecht University & CWI - Amsterdam, The Netherlands, menno.genseberger@wldelft.nl
[2]Utrecht University, The Netherlands, sleijpen@math.uu.nl
[3]Utrecht University, The Netherlands, vorst@math.uu.nl

We describe the domain decomposition technique for the two subdomain case. It can be generalized to more than two subdomains in a straightforward manner.

Let Ω be a domain over which some partial differential $\mathcal{L}\varphi = f$ is defined, together with appropriate boundary conditions on $\partial\Omega$. In order to compute numerical solutions, Ω is covered by a grid. The PDE is discretized accordingly, with unknowns defined on the grid points.
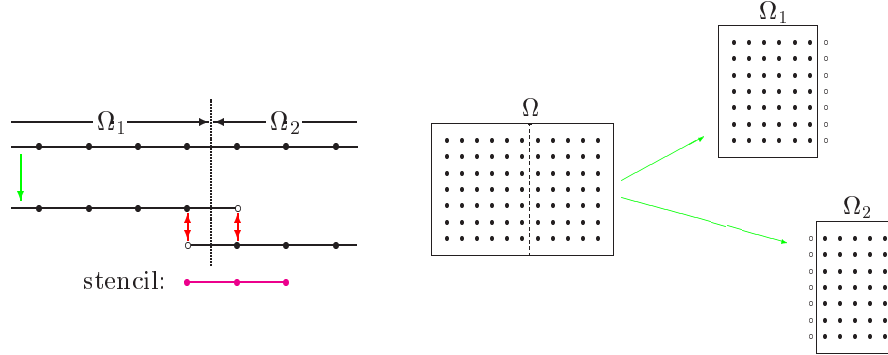

Figure 3.1: Decomposition in one (left picture) and two dimensions (right picture).

We decompose Ω in two nonoverlapping subdomains Ω_1 and Ω_2. The subdomains are covered by subgrids such that no splitting of the original discretized operator has to be made (see Figure 3.1). For that purpose additional grid points (the open bullets "$\circ$" in Figure 3.1) are introduced on the opposite side of the subgrids next to the internal interface between the subdomains. Since this introduces extra unknowns on the additional grid points, we must also provide extra equations that describe these extra unknowns. Furthermore, for the exact solution of the discretized PDE we want the function values on these additional points of one subgrid to be equal to the function values on the grid points of the other subgrid on the same location. Now, the *enhancement* consists of providing the original system with extra unknowns at the additional grid points and extra equations with precisely this property.

To do so, suppose we have ordered the discretized PDE in a linear system

$$\mathbf{B}\,\mathbf{y} = \mathbf{d}, \tag{3.1}$$

with unique solution and the following structure:

$$\begin{bmatrix} \mathbf{B}_{11} & \mathbf{B}_{1\ell} & \mathbf{B}_{1r} & \mathbf{0} \\ \mathbf{B}_{\ell 1} & B_{\ell\ell} & B_{\ell r} & \mathbf{0} \\ \mathbf{0} & B_{r\ell} & B_{rr} & \mathbf{B}_{r2} \\ \mathbf{0} & \mathbf{B}_{2\ell} & \mathbf{B}_{2r} & \mathbf{B}_{22} \end{bmatrix} \begin{bmatrix} \mathbf{y}_1 \\ y_\ell \\ y_r \\ \mathbf{y}_2 \end{bmatrix} = \begin{bmatrix} \mathbf{d}_1 \\ d_\ell \\ d_r \\ \mathbf{d}_2 \end{bmatrix}.$$

Here the labels $1, 2, \ell$, and r, respectively, refer to operations from/to and (un)knowns on subdomain Ω_1, Ω_2, and left, right from the interface, respectively. Subvector y_ℓ (y_r respectively) contains those unknowns on the left (right) from the interface that are coupled by the stencil both with unknowns in Ω_1 (Ω_2) and unknowns on the right (left) from the interface. This explains the zeros in the expression for matrix $\mathbf{B}$.

We enhance the linear system (3.1) to

$$\mathbf{B}_C\,\underline{\mathbf{y}} = \underline{\mathbf{d}} \tag{3.2}$$

which has the following structure:

$$
\begin{bmatrix}
\mathbf{B}_{11} & \mathbf{B}_{1\ell} & \mathbf{B}_{1r} & \mathbf{0} & \mathbf{0} & \mathbf{0} \\
\mathbf{B}_{\ell 1} & B_{\ell\ell} & B_{\ell r} & 0 & 0 & \mathbf{0} \\
\mathbf{0} & C_{\ell\ell} & C_{\ell r} & -C_{\ell\ell} & -C_{\ell r} & \mathbf{0} \\
\mathbf{0} & -C_{r\ell} & -C_{rr} & C_{r\ell} & C_{rr} & \mathbf{0} \\
\mathbf{0} & 0 & 0 & B_{r\ell} & B_{rr} & \mathbf{B}_{r2} \\
\mathbf{0} & \mathbf{0} & \mathbf{0} & \mathbf{B}_{2\ell} & \mathbf{B}_{2r} & \mathbf{B}_{22}
\end{bmatrix}
\begin{bmatrix}
\mathbf{y}_1 \\
y_\ell \\
\tilde{y}_r \\
\tilde{y}_\ell \\
y_r \\
\mathbf{y}_2
\end{bmatrix}
=
\begin{bmatrix}
\mathbf{d}_1 \\
d_\ell \\
0 \\
0 \\
d_r \\
\mathbf{d}_2
\end{bmatrix}.
\tag{3.3}
$$

Here $\tilde{y}_r$ ($\tilde{y}_\ell$ respectively) contains the unknowns at the additional grid points (the open bullets "∘" in Figure 3.1) of the subgrid for Ω_1 (Ω_2) on the right (left) of the interface. So, for the exact solution of (3.2) we want that $\tilde{y}_\ell = y_\ell$ and $\tilde{y}_r = y_r$. The only requirement for the extra equations in (3.3) that the submatrix

$$
C \equiv \begin{bmatrix}
C_{\ell\ell} & C_{\ell r} \\
C_{r\ell} & C_{rr}
\end{bmatrix},
$$

the *interface coupling matrix*, is nonsingular. For nonsingular C it can be proven ([5, Theorem 1]) that the solution of the enhanced system (3.2) is unique, $\tilde{y}_\ell = y_\ell$ and $\tilde{y}_r = y_r$ as required, and the restriction of this solution $\underset{\sim}{\mathbf{y}}$ to $\mathbf{y}$ is the unique solution of the original system (3.1).

However, we want to perform solves on the subgrids only. For that purpose we split the matrix of the enhanced system (3.2) as $\mathbf{B}_C = \mathbf{M} - \mathbf{N}$. Here $\mathbf{M}$ is the boxed part in (3.3) that does not map elements from one subgrid to the other subgrid. Note that compared to $\mathbf{M}$ the remainder $\mathbf{N}$ has a relatively small number of nonzero elements. (The rank of $\mathbf{N}$ equals the dimension of C which corresponds to the amount of virtual overlap that we have created. For a five point stencil in the two subdomain case the dimension of C is for instance $2n_i$, where n_i is the number of grid points along the interface.)

A simple iterative solution method for the splitting $\mathbf{B}_C = \mathbf{M} - \mathbf{N}$ is the Richardson iteration:

$$
\underset{\sim}{\mathbf{y}}^{(i+1)} = \underset{\sim}{\mathbf{y}}^{(i)} + \mathbf{M}^{-1}\left(\underline{\mathbf{d}} - \mathbf{B}_C\,\underset{\sim}{\mathbf{y}}^{(i)}\right).
\tag{3.4}
$$

Due to the splitting the iterates $\underset{\sim}{\mathbf{y}}^{(i)}$ of (3.3) are perturbed by errors. With $\mathbf{M}^{-1}\mathbf{B}_C = \mathbf{I} - \mathbf{M}^{-1}\mathbf{N}$ it can easily be verified that in each step these errors are amplified by the *error propagation matrix* $\mathbf{M}^{-1}\mathbf{N}$. Now, the idea is to use the degrees of freedom that we have created by the introduction of additional unknowns near the interface in order to damp the error components. Before we can perform this tuning of the interface coupling matrix C, we need to analyze the spectral properties of $\mathbf{M}^{-1}\mathbf{N}$ for the specific underlying PDE. For ordinary systems of linear equations originating from advection dominated problems this was done in [5, 4]. In §4 we describe and analyze the situation for the correction equation.

Besides the tuning of the interface coupling matrix we can further speed up the process for finding a solution of (3.3). The Richardson iteration uses only information from the last iterate for the computation of a new one. The process can be accelerated by interpreting the iterates as a Krylov subspace

$$
\mathcal{K}_m\left(\mathbf{M}^{-1}\mathbf{B}_C, \mathbf{M}^{-1}\underline{\mathbf{d}}\right) = \mathrm{span}\left(\mathbf{M}^{-1}\underline{\mathbf{d}}, \mathbf{M}^{-1}\mathbf{B}_C\,\mathbf{M}^{-1}\underline{\mathbf{d}}, \ldots, \left(\mathbf{M}^{-1}\mathbf{B}_C\right)^{m-1}\mathbf{M}^{-1}\underline{\mathbf{d}}\right)
$$

and computing an approximate solution for (3.3) with respect to $\mathcal{K}_m$.

In fact, in this way the Krylov method computes a solution for the *left* preconditioned equation

$$
\mathbf{M}^{-1}\mathbf{B}_C\,\underset{\sim}{\mathbf{x}} = \mathbf{M}^{-1}\left(\underline{\mathbf{d}} - \mathbf{B}_C\,\underset{\sim}{\mathbf{y}}^{(0)}\right),
\tag{3.5}
$$

where $\underset{\sim}{\mathbf{y}}^{(0)}$ is some initial guess ($\underset{\sim}{\mathbf{y}}^{(0)} = \mathbf{0}$ is convenient, but other good choices are possible as well) and a solution for (3.2) is computed from (3.5) via $\underset{\sim}{\mathbf{y}} = \underset{\sim}{\mathbf{y}}^{(0)} + \underset{\sim}{\mathbf{x}}$.

Note that *right* preconditioning is possible as well and has some nice additional properties. As it is slightly more complicated, we don't discuss it here but refer to [1, §3.2.4, §3.3.3].

4. The correction equation. In this section we describe and analyze the domain decomposition technique for the correction equation.
First it is shown how the correction equation is enhanced and how the preconditioner is incorporated. Then we pay attention to the spectrum of the error propagation matrix for a model eigenvalue problem. With this knowledge in mind, a strategy is developed for the tuning of the interface coupling matrix.

Similar to the enhancements (3.3) in 3, the following components of the correction equation have to be enhanced: the matrix $\mathbf{B} \equiv \mathbf{A} - \theta\,\mathbf{I}$ to $\mathbf{B}_C$, the correction vector $\mathbf{t}$ to $\underset{\sim}{\mathbf{t}}$, and the vectors $\mathbf{u}$ and $\mathbf{r}$ to $\underline{\mathbf{u}}$ and $\underline{\mathbf{r}}$, respectively. For the enhancement of the additional projection $\mathbf{P}$ see [1, §3.3.2].

The preconditioner $\mathbf{M}$ for $\mathbf{B}_C$ is constructed in the same way as in §3. In case of left preconditioning with $\mathbf{M}$ we compute approximate solutions to the correction equation from

$$\mathbf{P}'\,\mathbf{M}^{-1}\,\mathbf{B}_C\,\mathbf{P}'\,\underset{\sim}{\mathbf{t}} = \mathbf{P}'\,\mathbf{M}^{-1}\,\underline{\mathbf{r}} \quad \text{with} \quad \mathbf{P}' \equiv \mathbf{I} - \frac{\mathbf{M}^{-1}\,\underline{\mathbf{u}}\,\underline{\mathbf{u}}^*}{\underline{\mathbf{u}}^*\,\mathbf{M}^{-1}\,\underline{\mathbf{u}}}.$$

In [1, §3.4.3] the spectrum of the error propagation matrix is analyzed for the eigenvalue problem of an advection-diffusion operator with no cross terms and constant coefficients on two subdomains. We summarize the main results here.
The interface between the two subdomains Ω_1 and Ω is again in the y-direction. To facilitate the analysis, the discretized operator is written as a tensor product of one-dimensional discretized advection diffusion operators L_x and L_y: $L_x \otimes \mathbf{I} + \mathbf{I} \otimes L_y$. It turns out that the eigenvectors of the error propagation matrix show two typical types of behavior for the correction equation. This is illustrated in Figure 4.1.
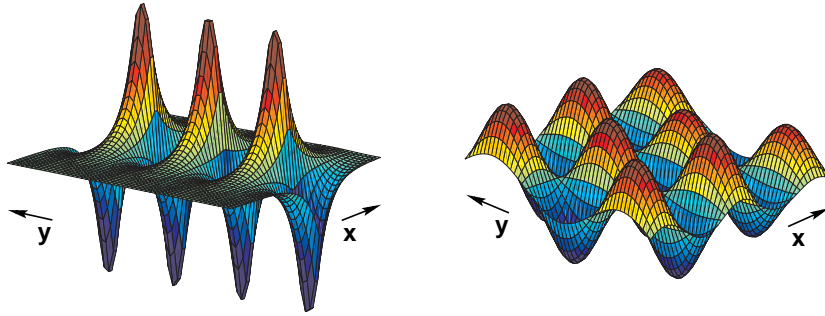

Figure 4.1: Typical eigenvectors of the error propagation matrix for the correction equation.

Parallel to the interface, all eigenvectors are coupled by eigenvectors of the one-dimensional operator L_y in the y-direction. Because of this, for the subblocks $C_{\ell\ell}$, $C_{\ell r}$, $C_{r\ell}$ and C_{rr} of the interface coupling matrix C we can take any linear combination of powers of L_y, for instance $C_{\ell\ell} = C_{rr} = \mathbf{I}$ and $C_{\ell r} = C_{r\ell} = \alpha\,\mathbf{I} + \beta\,L_y$. Here we are free to choose values for α and β, i.e. we can use these parameters for the minimization of the spectral radius of the error propagation matrix.
Perpendicular to the interface, however, there are differences. Most of the eigenvectors of the error propagation matrix show exponential behavior in the x-direction, the error grows exponentially fast when moving towards the interface (the left picture in Figure 4.1). A small number (this number depends on the location of the shift θ in the spectrum of matrix $\mathbf{A}$)

show harmonic behavior in the x-direction (the right picture in Figure 4.1), which has the disadvantage of being global.

For the eigenvectors of the error propagation matrix with exponential behavior in the x-direction we can estimate effective values for the interface coupling matrix C without specific knowledge of the subdomain size. In §5 we will see that this is of interest for more practical situations. For this reason we minimize the spectral radius of the error propagation matrix only with respect to these eigenvectors. With deflation the remaining eigenvectors, those with harmonic behavior in the x-direction, are controlled. We illustrate deflation by means of an example.

4.1. Deflation. Now we show, by example, how deflation improves the condition of the preconditioned correction equation. We consider θ equal to the 20th eigenvalue of the Laplace operator on a domain $[0, 1] \times [0, 1]$. The domain is covered by a 31×31 grid and decomposed in two equal subdomains.
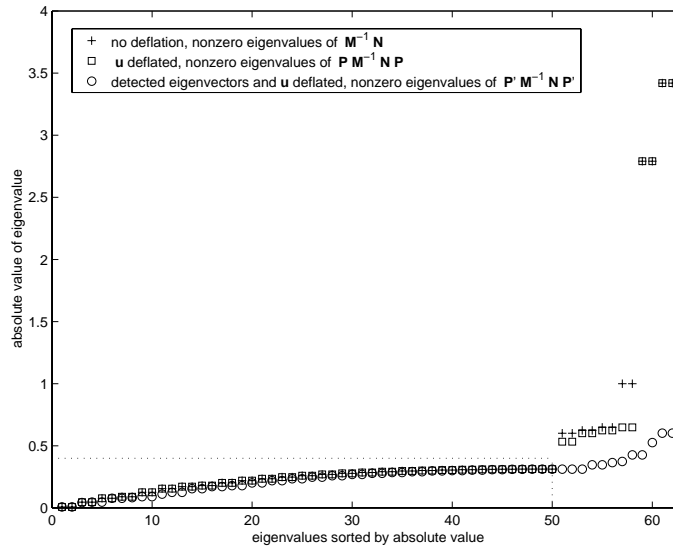

Figure 4.2: The effect of deflation.

In Figure 4.2 the nonzero eigenvalues of the error propagation matrix are shown for this situation.

Twelve eigenvectors of the error propagation matrix behave harmonic perpendicular to the interface. As we do not include them for the optimization, we do not necessarily damp these eigenvectors with the constructed interface coupling matrix as indicated by the twelve rightmost '+'-s (no deflation) in Figure 4.2.

Two of these eigenvectors are connected to the y-component of the eigenvector that corresponds to the 20th eigenvalue of the original eigenvalue problem: these eigenvectors can not be controlled at all with the interface coupling matrix because the operator $\mathbf{A}$ is shifted by this 20th eigenvalue and therefore singular in the direction of the corresponding eigenvector. In the correction equation the operator stays well-conditioned due to the projection $\mathbf{P}$ that deflates precisely this direction. Since the error propagator originates from the enhanced operator in the correction equation, this projection is actually incorporated in the error propagator and the '□'-s at positions 57 and 58 in Figure 4.2 show the positive effect. The other eigenvectors with harmonic behavior perpendicular to the interface can be controlled with information from the search subspace of Jacobi-Davidson itself: in practice one

starts the computation with the largest eigenvalues and when arrived at 20th one, the 19 largest eigenvalues with corresponding eigenvectors are already computed and will be deflated from the operator **B**. Deflation with these 19 already computed eigenvectors drastically reduces the absolute values, as the 'o'-s at the horizontal positions $51, \ldots, 56$ and $59, \ldots, 62$ show in Figure 4.2.

From this example we learned that deflation may help to cluster the part of the spectrum that we can not control with the coupling parameters, and therefore improves the conditioning of the preconditioned correction equation. The remaining part of the spectrum, that is the eigenvalues that are in control (indicated by the dotted lines in Figure 4.2), can be damped even more with a stronger optimized coupling.

5. Applications. With the results from the analysis for the two subdomain case with constant coefficients in §4 we can accurately estimate optimal interface coupling matrices C for more than two subdomains, variable coefficients, and complicated geometries.
As an illustration we give two numerical examples, for specific details we refer to [1].
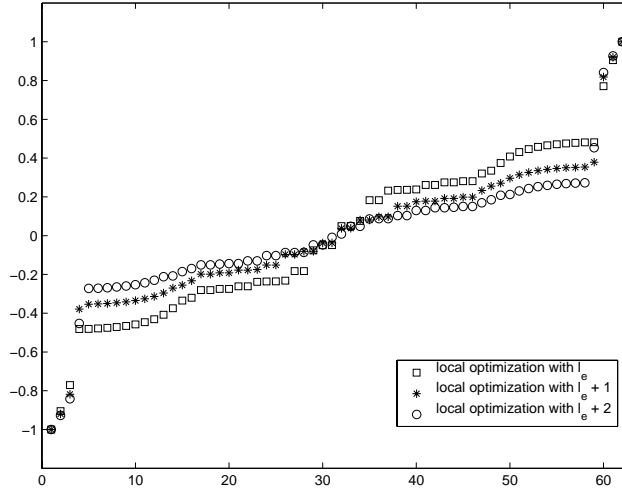

Figure 5.1: Eigenvalues of the error propagation matrix of the correction equation for an operator with a large jump.

5.1. Variable coefficients. In this example we illustrate the effectiveness of the determination of interface coupling matrices C for eigenvalue problems with variable coefficients.
Consider the following operator with a large jump:

$$\mathcal{L} \equiv \frac{\partial}{\partial x}[c(y)\frac{\partial}{\partial x}] + \frac{\partial}{\partial y}[c(y)\frac{\partial}{\partial y}] \ \text{ with } \ c(y) = \left\{ \begin{array}{c} 1 \text{ for } 0 \leq y < 0.25 \\ 1000 \text{ for } 0.25 \leq y < 0.75 \\ 1 \text{ for } 0.75 \leq y \leq 1 \end{array} \right.$$

defined on $[0, 2] \times [0, 1]$. We focus on the largest eigenvalue of this operator, the corresponding eigenvector is the most smooth one among all eigenvectors. The domain is decomposed into two equal subdomains with physical sizes $[0, 1] \times [0, 1]$ and $[1, 2] \times [0, 1]$, and covered by a 31×31 grid.

Based on a local optimization strategy [1, §4.3], which uses results of the constant coefficients case, we determined appropriate values for the interface coupling matrix. Figure 5.1

shows the eigenvalues of the corresponding error propagation matrix. It shows the effectiveness of C: smaller eigenvalues result in faster damping of the errors.

For the optimization three values of l_e are considered. This l_e marks the subdivision in harmonic and exponential behavior perpendicular to the interface of the eigenvectors of the error propagation matrix. For constant coefficients we were able to determine the precise, fixed value of l_e. For variable coefficients the value of l_e varies.

If we concentrate on the eigenvalues at the horizontal positions $4, 5, \ldots, 59$ in Figure 5.1, then we see that, compared to the local optimization with l_e (the '□'-s), these eigenvalues are closer to zero for the local optimization with $l_e + 1$ (the '∗'-s). So, for variable coefficients, the outcome of this experiment indicates that the value of l_e should not be chosen too sharp.

From the figure it can be concluded that, except for a couple of outliers at the horizontal positions $1, 2, 3, 60, 61$, and 62 (which can be controlled by deflation and/or the Krylov acceleration), the local optimization strategy yields an effective interface coupling matrix C.

5.2. More than two subdomains. For this example, we start with an eigenvalue problem that is defined on two square subdomains of equal size. The subdomains are covered by a 63×63 subgrid. The number of subdomains is increased by pasting a new subdomain of the same size. So we model a channel that becomes larger each time. With Jacobi-Davidson we compute an approximate solution of the eigenpair that corresponds to the largest eigenvector of the two-dimensional Laplace operator. Each step of Jacobi-Davidson we use 4 steps of the Krylov method GMRES [2] preconditioned with the preconditioner based on domain decomposition. Given a number of subdomains (first row in Table 5.1) we compare the total number of Jacobi-Davidson steps that are needed such that the ℓ_2-norm of the residual $\mathbf{r}$ of the approximate eigenvalue is less than 10^{-9} for three kinds of coupling: Neumann-Dirichlet coupling ("ad hoc" choice for C: Neumann boundary condition on the left: $C_{\ell\ell} = \mathbf{I}$, $C_{\ell r} = -\mathbf{I}$ and Dirichlet boundary condition on the right: $C_{r\ell} = C_{rr} = \mathbf{I}$), simple optimized coupling ($C_{\ell\ell} = C_{rr} = \mathbf{I}$ and $C_{\ell r} = C_{r\ell} = \alpha \mathbf{I}$), and stronger optimized coupling ("finetuning" of C: $C_{\ell\ell} = C_{rr} = \mathbf{I} + \gamma L_y$ and $C_{\ell r} = C_{r\ell} = \alpha \mathbf{I} + \beta L_y$). For the simple and stronger optimized coupling we estimate optimal values for C by doing as if the decomposition is in two subdomains only. With the results from the analysis in §3 we determine optimal values for C for the two subdomain case. Because only the eigenvectors of the error propagation matrix that damp exponentially when moving away from the interface are taken into account for the optimization, these values for C are also fairly good when the number of subdomains is larger than two.

number of subdomains	2	3	4	5	6
Neumann-Dirichlet coupling	5	9	19	21	22
simple optimized coupling	6	8	9	10	12
stronger optimized coupling	5	6	8	9	10

Table 5.1: Overall Jacobi-Davidson process on more subdomains for three different types of coupling.

From the table it can be concluded that a finer tuning of C pays off in the overall Jacobi-Davidson process. Note that for ease of presentation we used the Laplace operator here, experiments with more general advection-diffusion operators showed similar results.

<div align="center">REFERENCES</div>

[1] M. Genseberger. *Domain decomposition in the Jacobi-Davidson method for eigenproblems.* PhD thesis, Utrecht University, September 2001.

[2] Y. Saad and M. H. Schultz. GMRES: A generalized minimal residual algorithm for solving nonsymmetric linear systems. *SIAM J. Sci. Stat. Comp.*, 7:856–869, 1986.

[3] G. L. G. Sleijpen and H. A. van der Vorst. A Jacobi-Davidson iteration method for linear eigenvalue problems. *SIAM J. Matrix Anal. Appl.*, 17(2):401–425, 1996. Reappeared in SIAM Review 42:267–293, 2000.

[4] K. H. Tan. *Local coupling in domain decomposition*. PhD thesis, Utrecht University, 1995.

[5] K. H. Tan and M. J. A. Borsboom. On generalized Schwarz coupling applied to advection-dominated problems. In D. E. Keyes and J. Xu, editors, *Seventh International Conference of Domain Decomposition Methods in Scientific and Engineering Computing*, pages 125–130. AMS, 1994. Held at Penn State University, October 27-30, 1993.

[6] W. P. Tang. Generalized Schwarz splittings. *SIAM J. Sci. Stat. Comp.*, 13(2):573–595, 1992.